Observation of Discrete Energy Levels in a Quantum Confined System

L. L. A. Adams, B. W. Lang and A. M. Goldman

School of Physics and Astronomy, University of Minnesota,
116 Church St. SE, Minneapolis, MN 55455, USA
(Received textdate; Revised text)

Abstract

Low temperature scanning tunneling microscope images and spectroscopic data have been obtained on subnanometer size Pb clusters fabricated using the technique of buffer layer assisted growth. Discrete energy levels were resolved in current-voltage characteristics as current peaks rather than current steps. Distributions of peak voltage spacings and peak current heights were consistent with Wigner-Dyson and Porter-Thomas distributions respectively, suggesting the relevance of random matrix theory to the description of the electronic eigenstates of the clusters. The observation of peaks rather than steps in the current-voltage characteristics is attributed to a resonant tunneling process involving the discrete energy levels of the cluster, the tip, and the states at the interface between the cluster and the substrate surface. Shell document for REVTEX 4.

Random matrix theory (RMT) [1] is believed to describe the distribution of discrete energy states of quantum systems whose underlying classical behaviors are chaotic. In particular the Wigner-Dyson [2] and Porter-Thomas distributions [3] describe the level spacings and probability densities of the eigenfunctions, respectively. Features of Coulomb staircase tunneling characteristics have provided evidence of discrete energy levels in clusters of Au [4], InAs [5], and CdSe [6] studied using scanning probe techniques, and in Al grains [7] in fixed tunneling geometries. Peaks rather than steps have been found in quantum well geometries involving tunneling between electrodes, each characterized by discrete energy levels [8]-[10]. In this Letter, we report the observation of peaks in the I V characteristics of pancake shaped Pb clusters investigated using scanning probe techniques. We interpret these peaks as evidence of discrete energy levels. We find that the distribution of peak spacings, measured at different positions on the cluster, and which we associate with the distribution of energy levels spacings, , are consistent with the predictions of random matrix theory (RMT) in particular the orthogonal Wigner-Dyson distribution relevant to systems exhibiting time-reversal invariance symmetry.

It has also been possible to carry out a statistical analysis of values of the current found at these various peaks. The magnitude of the tunneling current is in part determined by the probability of an electron tunneling from the scanning tunneling microscope (STM) tip to the cluster. The histogram of current peaks is found to be consistent with Porter-Thomas statistics. The latter are believed to describe the distribution of probability densities of eigenfunctions characteristized by random matrices. Our hypothesis regarding the observation of peaks in the I V characteristics is that they are a consequence of a two-step tunneling process, from the tip to the cluster and then to a state with a narrow, well-defined, energy at the interface between the cluster and the semiconductor substrate.

Cluster fabrication was carried out in an ultra-high vacuum chamber using the technique of buffer layered assisted growth [11]. This growth chamber, which was equipped with Knudsen cells, was joined to the vacuum chamber of a commercial low temperature ultrahigh vacuum scanning tunneling microscope. Samples could be moved between chambers without breaking vacuum. Prior to the fabrication of clusters, the native oxide of the Si substrate was removed using a standard acid etch. Titanium/platinum electrodes were first deposited onto the substrate through a stainless steel mask using a separate electron beam evaporation system. The n-type (phosphorous doped) Si(111) wafer employed as a substrate, was miscut by 0.5 and had a room temperature bulk resistivity > 1000 cm, as specified by Virginia Semiconductor. After heating the substrate to 400 C in ultra-high vacuum for two hours, the substrate was cooled in the vacuum chamber using a flow-through cryostat. This was a two-stage process, first cooling with liquid nitrogen and then with liquid helium. Once the substrate temperature fell below 60 K, Xe gas was absorbed on its surface to produce a four monolayer thick film. Subsequently a Pb film with a nominal thickness of 0.2A, as measured by a calibrated quartz crystal monitor, was deposited onto the adsorbed Xe layer. Clusters were then formed on the substrate by desorbing the Xe layer as the sample temperature gradually approached room temperature. The sample was then transferred to the STM chamber without breaking vacuum.

Chemically etched W tips were used to perform the measurements. These were tested in situ by imaging a cleaved graphite surface and achieving atomic resolution. This was done prior to obtaining topographical and spectroscopic information about the clusters. All spectra were obtained during topographical imaging by interrupting the STM feedback and working in constant height mode. However I V characteristics were acquired in two different ways: either by stopping the scan over a particular site on a cluster and then sweeping the bias voltage, or automatically acquiring data at every raster point in a topographical scan. There was no apprecia-

ble difference between sets of data obtained in these two different ways.

The inset in Fig.1 displays a topographical trace obtained using a STM illustrating several clusters on top of a Si substrate. It is important to note that the clusters that exhibit peaks in their I V characteristics were effectively pancake shaped, with diameters on the order of 3 nm and heights between 0.3 and 1.5 nm. The main part of Fig.1 shows a typical plot of the I V characteristics at a particular location on one of these clusters. The data were obtained at a temperature of 4.2 K, which is low enough that sharp features are resolvable. The typical width of a peak was approximately 5 meV. The cluster's "image" size for this particular example was 3.7 nm in length, 2.6 nm in width and 0.7 nm in height. (The actual cluster size is likely to be smaller due to convolution effects associated with the STM tip. [11]) To interpret this data the hypothesis that the peaks resulted from resonant tunneling involving the discrete electronic energy levels of the cluster was adopted. The results of a statistical analysis of the data assuming that this is the case, will be described first. The issue as to why this might be true, and why the energy levels appear as peaks rather than steps in the I V characteristic will then be discussed.

In order to obtain statistical data, it is important to note that the observed I V characteristics vary with position across a cluster as shown in Fig.2 where the tunneling current obtained at a fixed bias voltage as a function of position is displayed. By measuring the I V characteristics at regular positions on a specific cluster, a large data set of peak positions and peak heights can be obtained for the given cluster. After acquiring data at approximately 280 locations on a specific cluster histograms of peak spacings and peak heights were generated using the program ROOT [12].

The histogram of normalized peak spacings, (normalized to the mean spacing of each individual trace) was then fit by the distribution function

$$P(s) = b\, s^{\ } \exp(-a\, s^{c}) \qquad (1)$$

Here the normalized mean spacing, s, is simply $= h\ i$, with representing the level spacing and $h\ i$ the mean spacing. Equation 1 can represent the orthogonal (= 1), unitary (= 2) and symplectic (= 4) ensembles [13] that correspond to processes with different symmetries. The orthogonal case corresponds to time reversal symmetry being preserved in the absence of a magnetic field and describes the results presented here. In the statistical analysis of this histogram fits to Wigner-Dyson, Poisson, Gaussian, and Lorentzian distributions were made. From the values of ^{2} (not shown) it is clear that the Wigner-Dyson distribution provides the best fit to the data with $a = =4; b = =2$ and $c = 2$. In Fig.3, the histogram of peak spacings for this cluster, showing the Wigner-Dyson and Poisson fits is plotted.

A similar statistical analysis of the histogram of current peak heights was also carried out. The following form [14],

$$P(I) = a \left(\frac{I}{< I >}\right)^{b} \exp\left(c\, \frac{I}{< I >}\right) \qquad (2)$$

was fit to the data, where I is the peak current and $< I >$ the mean peak current. In this analysis, parameters specific to the Porter-Thomas and Poisson distributions, which were deemed relevant, were used. The Porter-Thomas distribution (with $a = (2\ )^{\frac{1}{2}}; b = 1=2$ and $c = 1=2$) provided a somewhat better fit to the data than the Poisson distribution. Figure 4 shows a plot of the histogram along with curves associated with the best fits of the Porter-Thomas and Poisson distributions. The results of this analysis support the interpretation that these measurements are yielding spectroscopic information relating to the energy levels.

We now turn to the issue of why peaks rather than steps are found in the I V characteristics of the clusters. It is known that there are interface states and Fermi level pinning at epitaxial Pb/Si(111) interfaces involving n-type Si [15]. One such state pins the Fermi level just above the valence band minimum. This state has no measurable dispersion. Although the present configuration is not one in which Pb clusters were grown epitaxially on Si, one might expect to find an interface state of this sort. The data, involving peaks in the I V characteristics rather than steps, would be consistent with a picture in which electrons tunnel into the cluster from the STM tip and out of the cluster into the nearly dispersionless interface state. The surface of the substrate is replete with clusters so that there is likely to be a continuous distribution of conductive interface states, resulting in a conducting path connecting a particular cluster to the Pt electrodes.

As the voltage between the STM tip (at virtual ground) and the Pt electrodes on the substrate is varied, the narrow band interface state is tuned through the various energy levels of the cluster. The measurements are made with the STM tip at a particular position so that tunneling into the cluster involves electrons at the Fermi surface of the tip with the nearest unoccupied eigenstate of the cluster. The values of current at the peaks will reflect the distribution of tunneling probabilities, which are proportional to the square of the matrix elements for tunneling between the tip and the discrete eigenstates of the cluster. Although these eigenstates are extended throughout the cluster, their amplitudes can be a function of position, explaining the position dependence of the I V characteristics [16], and explaining why varying the position of the tip results in a large set of curves, with position-dependent peak spacings and peak heights. When taken in aggregate this data will reflect the statistical properties of the eigenstates of the cluster. Tunneling

out of the cluster would involve the eigenstate whose energy is matched with that of the interface state. As will be discussed below, this need not be the same state as that involved in the "tunneling in" process. The spectrum of discrete energy levels of the clusters would be explored by changing the voltage between the STM tip and the interface state.

An important issue is the role of charging energy in the proposed two-step tunneling process. Estimates assuming either two or three dimensional geometries exceed the values of the mean level spacing, suggesting that charge transport involves inelastic co-tunneling in which electrons tunnel into the cluster to a particular state and tunnel out from a different one, with no net charge being added to the cluster during the process [17]-[18]. Since in this picture the eigenstate amplitudes are position dependent, the threshold for resonant tunneling at a particular location, and thus the voltage of the first peak, depends upon the energy of that eigenstate relative to the Fermi energy of the tip. As a consequence the voltage at which the first peak is found can be position dependent, and the relevant physical quantities are the spacings between peaks rather than the voltages at which they were found. Normalized spacings were used in the analysis as a matter of convenience. Additional theoretical work is needed to elaborate on this hypothesis which appears to be central to understanding this data.

An estimate of the mean level spacing can be made using the nearly free electron model. In both the two-dimensional and three-dimensional cases, the discrete particle-in-the-box energy levels' estimate is determined from the size of the particle and the continuum density of states at the Fermi energy. For a Pb cluster of dimensions 3.7 nm in length, 2.6 nm in width and 0.7 nm in height, an estimate of the mean level spacing is 22 meV (two-dimensional) and 7 meV (three-dimensional). The experimental measured mean level spacing is $h\ i = 13{:}4$ meV for this cluster. It is noted that these values are an order of magnitude bigger than the thermal broadening energy at 4.2 K ($3{:}5\ k_B T \ s\ 1{:}3$ meV) and the energy gap of superconducting Pb which is $s\ 1$ meV. For this reason one would not expect to observe features in the tunneling characteristic associated with superconductivity.

The clusters which exhibit discrete energy levels described here were all extremely small and very thin and irregular in shape. They were effectively two dimensional quantum dot configurations. Although the explanation of the current peaks presented above is not substantiated by detailed surface and interface measurements, the distributions of the peak spacings and peak heights are consistent with expectations for a system exhibiting chaotic dynamics of discrete energy levels, probed by resonant tunneling. This provides support for the proposed mechanism. The level spacings are governed by the orthogonal Wigner-Dyson distribution, appropriate to a system in which time-reversal symmetry is not broken, as would be expected in zero magnetic field. The intensities of the tunneling current are found to satisfy a Porter-Thomas distribution.

We acknowledge valuable discussions with Alex Kaminev and Leonid Glazman. We thank Beth Masimore for help with the initial analysis of the data. This work was supported by the US Department of Energy under grant DE-FG02-02ER46004.

[1] M. L. Mehta, Random Matrices, 2nd ed., (Academic Press, London, 1991).
[2] Wigner, in Proc. Canadian Mathematical Congress, (Univ. of Toronto Press, Toronto, 1957); F. J. Dyson, J. Math. Phys. 3, 140 (1962).
[3] C. E. Porter, Statistical Theory of Spectra: Fluctuations, (Academic, New York 1965); R. G. Thomas and C. E. Porter, Phys. Rev. 104, 483 (1956).
[4] B. Wang et al., Phys. Rev. B 63, 035403-1 (2000).
[5] U. Banin, Y. Cao, D. Katz and O. Millo, Nature 400, 542 (1999).
[6] E. P. A. M. Bakkers, Z. Hens, L. P. Kouwenhoven, L. Gurevich and D. Vanmaekelbergh, Nanotechnology 13, 258 (2002).
[7] D. C. Ralph, C. T. Black and M. Tinkham, Phys. Rev. Lett. 74, 3241 (1995).
[8] L. L. Chang, L. Esaki, and R. Tsu, Appl. Phys. Lett. 24, 593 (1974).
[9] M. Tewordt, et al., Appl. Phys. Lett. 60, 595 (1992).
[10] N. C. van der Vaart et al., Phys. Rev. Lett. 74, 4702 (1995).
[11] L. Huang, S. J. Chey and J. H. Weaver, Phys. Rev. Lett. 80, 4095 (1998).
[12] http://root.cern.ch/
[13] D. A. Rabson, B. N. Narozhny and A. J. Millis, Phys. Rev. B 69, 054403-1 (2004).
[14] E. Runge and R. Zimmermann, Phys. Stat. Sol. (B) 221, 269 (2000).
[15] H. H. Weitering, A. R. H. F. Ettema and T. Hibma, Phys. Rev. B 45, 9126 (1992).
[16] K. Nakamura, Quantum Chaos-A New Paradigm of Nonlinear Dynamics, (Cambridge University Press, Cambridge, 1993).
[17] M. V. Feigelman and A. S. Ioselevich, preprint, cond-mat/0502481 (2005).
[18] L. I. Glazman and M. Pustilnik, preprint, cond-mat/0501007 (2005).

Figure 1 Tunneling current versus voltage at $T = 4.2$ K. Tunneling is from a tungsten STM tip into a Pb cluster. Inset: 30.0 nm x 30.0 nm image of Pb clusters grown by a buffer layer assisted growth technique. This image was obtained using a bias voltage of -3.0 V with a tunneling current of $2.0 \quad 10^{9}$ A.

Figure 2 Tunneling current as a function of position in the plane of a cluster at a fixed applied voltage of 17

meV at T = 4.2 K.

Figure 3 Histogram of peak spacings. The solid curve is the fit for the Wigner-Dyson distribution. The dotted line represents the fit for the Poisson distribution. There are 413 peak spacings that comprise this histogram normalized to the mean voltage spacing.

Figure 4 Histogram of peak heights. The solid curve is the fit for the Porter-Thomas distribution. The dotted line represents the fit for the Poisson distribution. There are 851 peak heights that comprise the histogram normalized to the mean peak current.

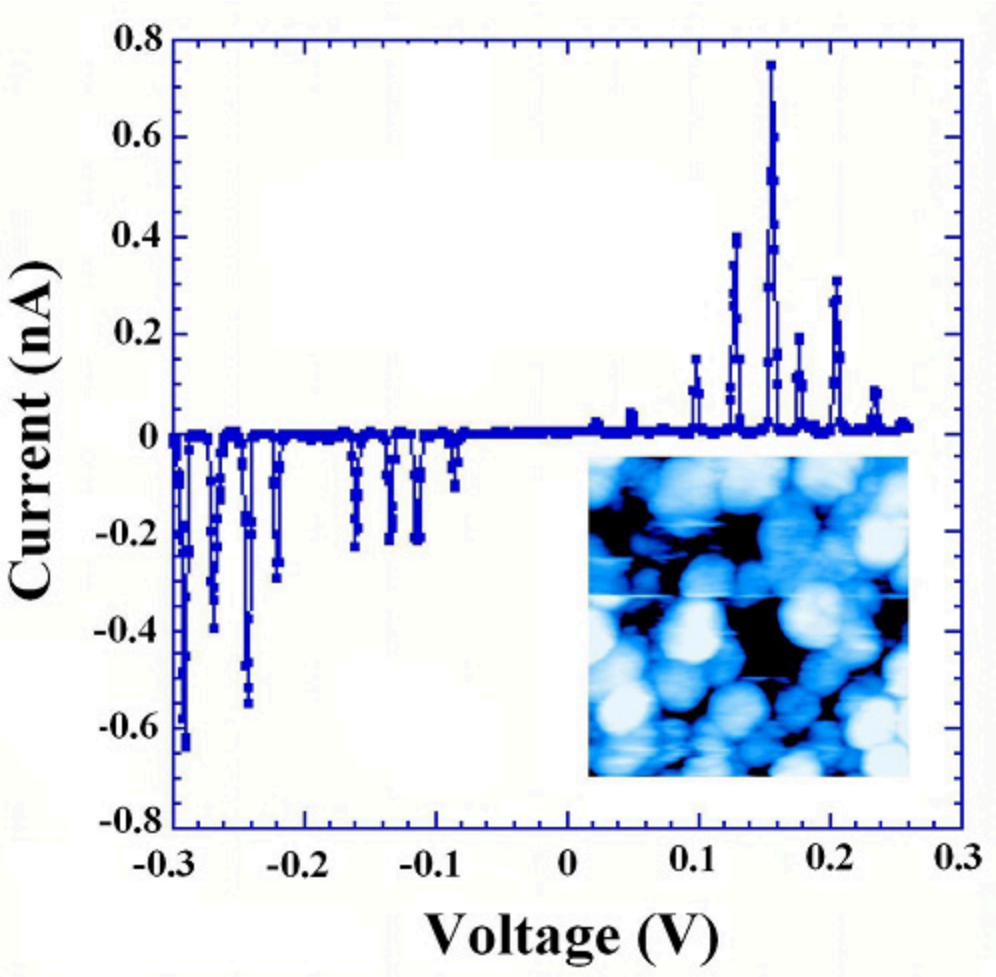
0.8
0.6
0.4
0.2
0
-0.2
-0.4
-0.6
-0.8
-0.3
-0.2
-0.1
0
0.1
0.2
0.3
Current (nA)
Voltage (V)

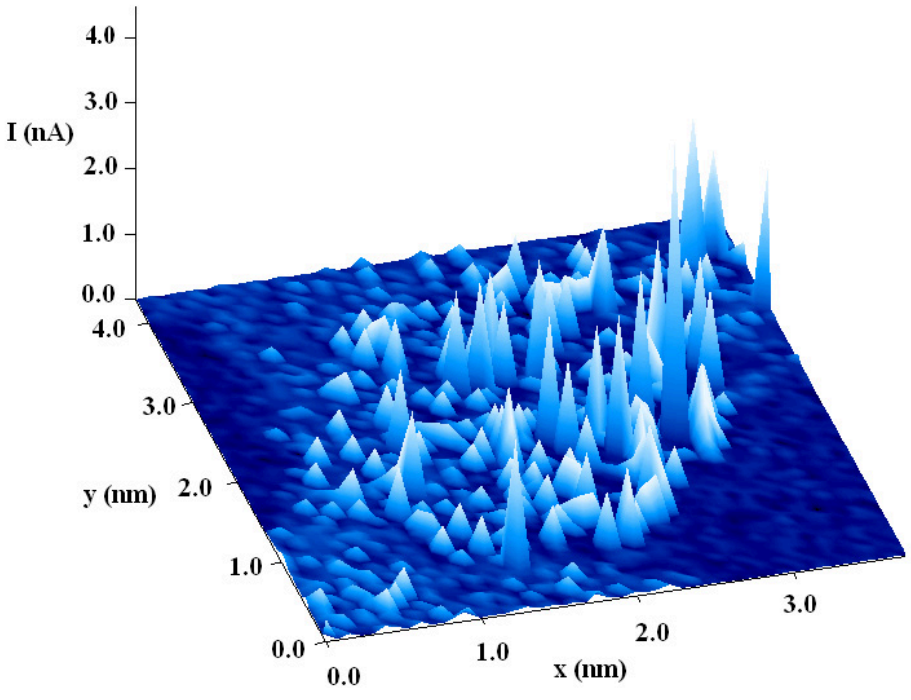
I (nA)
4.0
3.0
2.0
1.0
0.0
y (nm)
4.0
3.0
2.0
1.0
0.0
0.0
1.0
2.0
3.0
x (nm)

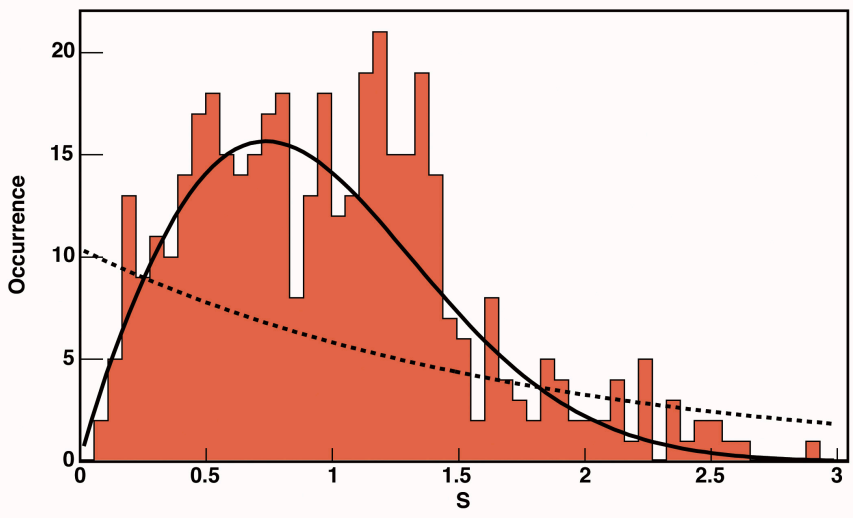
Occurrence
S
0
5
10
15
20
0
0.5
1
1.5
2
2.5
3

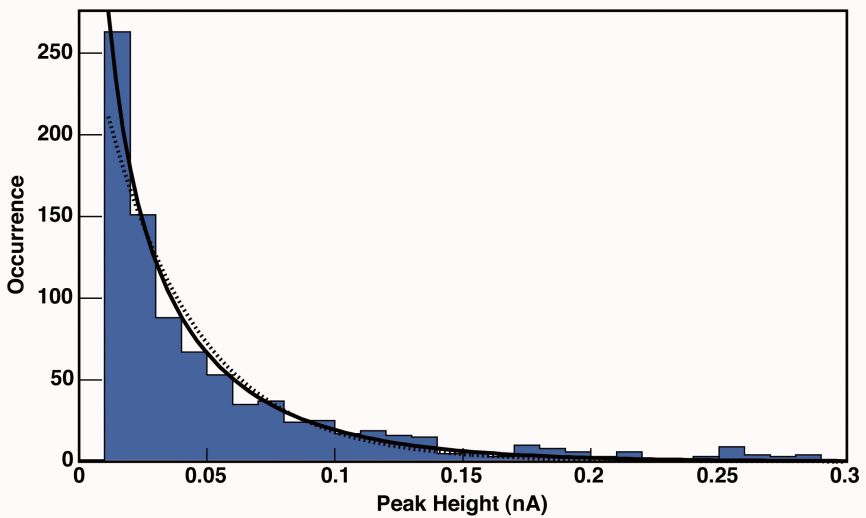
Occurrence
250
200
150
100
50
0
0
0.05
0.1
0.15
0.2
0.25
0.3
Peak Height (nA)